NONLINEAR LOAD DEFLECTION CHARACTERISTICS OF A REACTOR FUEL BUNDLE

H. D. FISHER

Reactor Engineering Department, Division 9485,
Combustion Engineering, Inc., 1000 Prospect Hill Road, Windsor, Connecticut 06095, U.S.A.

SUMMARY

In a seminal paper, L. L. Barinka, in J. Engineering for Industry, Nov. 1971, 1255-1260, described a coupled tubular structure model for use in calculating the transverse deflection of statically loaded reactor fuel bundles. Nonlinear factors included in his analysis are the loss of axial constraint due to tube slippage and a reduction in rotational constraint due to nonlinear spring coupling.

Employing a lucid free body diagram of a bundle segment, the present study demonstrates that for bundles consisting of two tube types (the typical application in the nuclear industry) a physically realistic model for the calculation of static deformation is described by a system of N equations in N unknowns where N equals 12 rather than 16 as in Barinka's work. Inspection of equations (12a) and (12b) of Barinka discloses the need for refining the theory for bundles composed of more than one tube type. Moment equilibrium of the spacer grid dictates that the *sum* of equations (12a, $r' < f_0$) or (12b, $r' \geq f_0$) for all tube types is equal to zero rather than each contribution for a particular tube type. Specifically, for two tube types the equation (Barinka's notation is employed here with r' assumed to be greater than f_0)

$$[\sum^{N_1} r'Z + \sum^{N_2} f_0 Z - \sum^{N} m']_{\text{TYPE 1}} + [\sum^{N_1} r'Z + \sum^{N_2} f_0 Z - \sum^{N} m']_{\text{TYPE 2}} = 0 \qquad (1)$$

replaces the two equations (equations 12b) obtained by setting each of the two bracketed expressions above to zero.

The replacement of equations (12b) by (1) results in 15 equations in 16 unknowns. The number of unknowns is now reduced to 12 by observing that shearing deformation is governed by rigid coupling between the two types of rods and the grid. Therefore, the total resultant shearing force $Q1_i(Q2_i)$ in type 1 (type 2) rods, as well as the shearing force per rod $q1_i(q2_i)$, is determined as indicated in equations (8-10) of Halliday and Horvay, SMIRT-3 paper D 1/11.

A review of the remaining 15 equations from Barinka's work shows that computation of $q1_i$ and $q2_i$ as indicated above corresponds to deleting three of the 15 governing equations. Hence a system of 12 equations in 12 unknowns is sufficient to describe the static deformation of a fuel bundle containing two rod types.

In addition to correcting Barinka's analysis and indicating restrictions inherent in first order theory, this study extends the previous formulation to symmetrically loaded fuel bundles restrained by rotational springs with spring modulus K (K=0 is the case investigated by Barinka i.e. pinned ends). Employing an iterative technique similar to a procedure derived by Halliday and Horvay, numerical results are obtained which demonstrate that the end moments required to produce a specified end fixity cannot be determined from elementary beam theory. For a fuel bundle containing two types of rods and characterized by specific values of KX, Kθ, f_0 and m_0, the utility of the analysis as a design tool is demonstrated by presenting load-deflection curves (determined via a computer code) corresponding to end support conditions ranging from clamped-clamped to pinned-pinned.

1. INTRODUCTION

Experimental studies have demonstrated that nonlinearity is present in the load-deflection curve obtained from a fuel bundle subjected to static transverse loads. This paper describes an analytic method for simulating the nonlinear load-deflection behavior in fuel bundles restrained by specified boundary conditions which range from pinned-pinned to clamped-clamped. The analysis forms the basis of a FORTRAN program, the DASAB code, which enables the PWR structural designer to determine the critical design parameters in a given application. Nonlinear physical mechanisms described in the present model are the decrease in the axial restraining force produced by fuel tube slippage and the reduction in moment constraint with increasing angular rotation. The analysis discussed here has been extended to include bundles with asymmetric loading and/or geometry. Because the axial location of the point of maximum deflection must be ascertained by trial and error in the asymmetric case, the complexity of the analysis is significantly increased. For this reason, a description of the asymmetric formulation will be the subject of a separate paper.

2. ANALYSIS

A consistent segment model of the reactor fuel bundle is obtained by determining the shear $Q_{j,i}$ and moment $M_{j,i}$ (See Nomenclature) acting at each grid location from overall equilibrium of the bundle. For illustrative purposes a fuel bundle consisting of three layers of tubes (the simplest symmetric configuration with tubes situated away from the neutral axis) is shown in Figure 1. Here A1-B1, A2-B2 and A3-B3 represent the lengths of the respective tubes, the corresponding cross sections on which coupling of the tubes to the grids occurs are indicated by C1, C2 and C3 and the grid is represented by D1-D2-D3. The arrows in Figure 1 show the positive direction of the corresponding variables. The division of $Q_{j,i}$ and $M_{j,i}$ between the grid and the tubes at a given station is ascertained by employing the following assumptions:

1. The connection joining the tubes and the grid in the vertical direction is rigid ($q^c_{j,i}=0$).
2. The segment shear ($Q_{j,i}$) and moment ($M_{j,i}$) are shared equally by all like tubes of the assembly.
3. The fuel bundle is not subjected to axial loading and the neutral axis is inextensional.
4. The rigidity of the spacer grids is sufficient to insure that they rotate as plane sections.
5. All like tubes undergo identical transverse and rotary deformation.

Assumptions 2 through 5 were first employed in [1].

As indicated in Figure 2, the concentrated forces ($r^h_{j,i}$ and $q_{j,i}$) and the concentrated moment ($m_{j,i}$) are produced across the thickness of an individual tube, whereas the interaction force ($r^{h-}_{j,i}$) and the interaction moment ($m^{c-}_{j,i}$) are generated on the exterior surface of a given tube. The distribution (See Figure 1) of the imposed segment load ($Q_{j,i}/N_j$) and the imposed segment moment ($M_{j,i}/N_j$) between interior ($r^h_{j,i}, q_{j,i}, m_{j,i}$) and exterior ($r^{h-}_{j,i}, m^{c-}_{j,i}$) force and moment is dictated by the equilibrium and compatibility equations derived below. The axial and rotational slippage models utilized in the present study are indicated in Figures 3 and 4, respectively. The relationship between the interaction force $r^{h-}_{j,i}$ and the relative displacement is identical to that employed in [1]. The bilinear spring model for rotational coupling described in [1] has been extended to include as many as five segments (the number employed in a given analysis is designated via an input parameter in the DASAB computer code).

The governing equations will be derived assuming that the reactor fuel bundle has a symmetrical cross section and that it is composed of two types of tubes (fuel rods and guide tubes). Twelve equations in twelve unknowns are required to compute the transverse deformation that results from the application of concentrated and/or uniform symmetric loading to this type of fuel bundle. The derivation of these equations is similar to that of [1]. However, significant modifications to these equations are required to describe the equilibrium of the spacer grids and the distribution of the segment shearing force between the fuel rods and the guide tubes.

From Figure 1 and assumptions 1 and 2, the distribution of the imposed segment loads and moments between the internal and external forces and moments acting on a guide tube (denoted by subscript g) and a fuel rod (denoted by a subscript f) at a given axial station (denoted by subscript i) is described by the equations (the superscript h denotes that the indicated variable is dependent on the transverse location on the cross section).

$$r^h_{g,i} - r^{h'}_{g,i} = 0 \tag{2a}$$

$$r^h_{f,i} - r^{h'}_{f,i} = 0 \tag{2b}$$

$$q_{g,i} = Q_{g,i}/N_g \tag{3a}$$

$$q_{f,i} = Q_{f,i}/N_f \tag{3b}$$

$$m_{g,i} - m'_{g,i} = \frac{M_{g,i}}{N_g} \tag{4a}$$

$$m_{f,i} - m'_{f,i} = \frac{M_{f,i}}{N_f} \tag{4b}$$

From assumption 1 and Halliday and Horvay [2], the total resultant shear force transmitted to the guide tubes and fuel rods, respectively, is

$$Q_{g,i} = \frac{E_g I_g Q_i}{(N_g E_g I_g + N_f E_f I_f)} \tag{5a}$$

$$Q_{f,i} = \frac{E_f I_f Q_i}{(N_g E_g I_g + N_f E_F I_f)} \tag{5b}$$

Substituting (5a) into (3a) and (5b) into (3b), the shearing force in the individual guide tubes and fuel rods is given by

$$q_{g,i} = \frac{E_g I_g Q_i}{N_g (N_g E_g I_g + N_f E_f I_f)} \tag{6a}$$

$$q_{f,i} = \frac{E_f I_f Q_i}{N_f (N_g E_g I_g + N_f E_f I_f)} \tag{6b}$$

Utilizing the equations for the deflection and rotation produced in a cantilever beam subjected to a uniform load over the segment span together with a force and moment acting at the end, the transverse and angular deformations of the guide tubes and fuel rods are given by

$$\Delta Y_{g,i} = \frac{L_i^3}{3E_g I_g} q_{g,i} + \frac{L_i^2 m_{g,i}}{2E_g I_g} - \frac{L_i^4 w_g}{8N_g E_g I_g} \tag{7a}$$

$$\Delta Y_{f,i} = \frac{L_i^3}{3E_fI_f} q_{f,i} + \frac{L_i^2 m_{f,i}}{2E_fI_f} - \frac{L_i^4 w_f}{8N_fE_fI_f} \quad (7b)$$

$$\Delta\theta_{g,i} = \frac{L_i^2}{2E_gI_g} q_{g,i} + \frac{L_i m_{g,i}}{E_gI_g} - \frac{L_i^3 w_g}{6N_gE_gI_g} \quad (8a)$$

$$\Delta\theta_{f,i} = \frac{L_i^2}{2E_fI_f} q_{f,i} + \frac{L_i m_{f,i}}{E_fI_f} - \frac{L_i^3 w_f}{6N_fE_fI_f} \quad (8b)$$

The axial deformation of the guide tubes and fuel rods is obtained from the equations

$$\Delta X^h_{g,i} = \frac{L_i r^h_{g,i}}{A_gE_g} \quad (9a)$$

$$\Delta X^h_{f,i} = \frac{L_i r^h_{f,i}}{A_fE_f} \quad (9b)$$

The coupling forces between the tubes and the grid (See Figure 3) are given by

$$r^{h'}_{g,i} = KX_g(\delta X^h_{g,i} - \Delta X^h_{g,i}) \qquad \text{No slipping of the guide tubes} \quad (10a)$$

For $|r^{h'}_{f,i}| \leq f_o$ (10b)

$$r^{h'}_{f,i} = KX_f(\delta X^h_{f,i} - \Delta X^h_{f,i})$$

Otherwise

$$r^{h'}_{f,i} = f_o \text{ for } r^{h'}_{f,i} > 0$$

$$r^{h'}_{f,i} = f_o \text{ for } r^{h'}_{f,i} < 0$$

From Figure 4, the equations governing the coupling moments are

$$m_{g,i} = K\theta l_g (\delta\theta_{g,i} - \Delta\theta_{g,i}) \qquad \text{No reduction of rotational constraint for guide tubes} \quad (11a)$$

For $|m'_{f,i}| \leq m_o(2)$ (11b)

$$m'_{f,i} = K\theta l_f(\delta\theta_{f,i} - \Delta\theta_{f,i})$$

For $m_o(2) < m'_{f,i} \leq m_o(3)$

$$m'_{f,i} = K\theta l_f(\delta\theta^{p2}_{f,i} - \Delta\theta^{p2}_{f,i}) + K\theta 2_f[(\delta\theta_{f,i} - \Delta\theta_{f,i}) - (\delta\theta^{p2}_{f,i} - \Delta\theta^{p2}_{f,i})]$$

For $-m_o(3) \leq m'_{f,i} < -m_o(2)$

$$m'_{f,i} = K\theta 1_f(\delta\theta_{f,i}^{n2} - \Delta\theta_{f,i}^{n2}) + K\theta 2_f[(\delta\theta_{f,i} - \Delta\theta_{f,i}) - (\delta\theta_{f,i}^{n2} - \Delta\theta_{f,i}^{n2})]$$

Similar equations can be written for the remaining number of segments desired on the curve shown in Figure 4.

From Figure 1, the rigidity and equilibrium constraints on the grid require that

$$\delta X_{g,i}^h = - Z_{g,i}^h \, \delta\theta_{g,i} \tag{12a}$$

$$\delta X_{f,i}^h = - Z_{f,i}^h \, \delta\theta_{f,i} \tag{12b}$$

$$- \sum_{h=1}^{NRG} N_g^h \, r_{g,i}^{h'} Z_{g,i}^h - \sum_{h=1}^{NRF} N_f^h \, r_{f,i}^{h'} Z_{f,i}^h + \sum_{h=1}^{NRG} N_g^h \, m'_{g,i} + \sum_{h=1}^{NRG} N_f^h \, m'_{f,i} = 0 \tag{13}$$

From (2a),(2b),(9a),(9b),(10a),(10b) and (12), the axial force in the guide tubes and fuel rods is expressed as

$$r_{g,i}^{h'} = \frac{-(KX_g) Z_{g,i}^h \, \delta\theta_{g,i}}{\left[1 + \frac{L_i(KX_g)}{A_g E_g}\right]} \tag{14a}$$

For $|r_{f,i}^{h'}| \leq f_o$

$$r_{f,i}^{h'} = \frac{-(KX_f) Z_{f,i}^h \, \delta\theta_{f,i}}{\left[1 + \frac{L_i(KX_f)}{A_f E_f}\right]} \tag{14b}$$

Otherwise

$r_{f,i}^{h'} = f_o$ for $r_{f,i}^{h'} > 0$

$r_{f,i}^{h'} = -f_o$ for $r_{f,i}^{h'} < 0$

Substituting (14a) and (14b) into (13), moment equilibrium is described by

$$N_{g,i} m'_{g,i} + N_{f,i} m'_{f,i} = \frac{-(KX_g)\delta\theta_{g,i}}{\left[1 + \frac{L_i(KX_g)}{A_g E_g}\right]} \sum_{h=1}^{NRG} (Z_{g,i}^h)^2 N_g^h$$

$$- \frac{(KX_f)\delta\theta_{f,i}}{\left[1 + \frac{L_i(KX_f)}{A_f E_f}\right]} \sum_{h=NRS+1}^{NRF-NRS} (Z_{f,i}^h)^2 N_f^h \tag{15}$$

$$+ 2 \sum_{h=1}^{NRS} f_o (Z_{f,i}^h) N_f^h$$

where, in the last term on the RHS of (15), the factor 2 is required to include the contribution from the slipped tubes with a positive Z coordinate.

An additional moment equilibrium equation is derived by observing that the total moment on the cross section (M_i) is the sum of the resultant moment in the guide tubes ($M_{g,i}$) and the resultant moment in the fuel rods ($M_{f,i}$) or

$$M_i = M_{g,i} + M_{f,i} \tag{16}$$

As in [1], compatibility of the resulting deformations is enforced by requiring that the location of the spacer grid at the end of segment i is the same in the two coordinate systems. For small deflections and rotations of the elastic curve (See-Popov [3]), imposing the above condition on the vertical displacement of the grid results in

$$\Delta Y_{g,i} + L_i\theta_{g,i-1} + Y_{g,i-1} = \Delta Y_{f,i} + L_i\theta_{f,i-1} + Y_{f,i-1} \tag{17}$$

Equating the two expressions for the angular rotation of the grid yields

$$\delta\theta_{g,i} + \theta_{g,i-1} = \delta\theta_{f,i} + \theta_{f,i-1} \tag{18}$$

This completes the derivation of the governing system of equations. After substituting the values of $q_{g,i}$ and $q_{f,i}$ as given by (6a) and (6b) into (7a), (7b) (8a) and (8b), the moments and deformations of the two types of tubes are determined by the simultaneous solution of the twelve equations (4a),(4b),(7a),(7b), (8a),(8b)(11a),(11b),(15),(16),(17) and (18) in the twelve unknowns $\Delta Y_{g,i}$, $\Delta Y_{f,i}$ $\Delta\theta_{g,i}$,$\Delta\theta_{f,i}$,$\delta\theta_{g,i}$,$\delta\theta_{f,i}$,$m_{g,i}$,$m_{f,i}$,$\bar{m}_{g,i}$,$\bar{m}_{f,i}$,$M_{g,i}$ and $M_{f,i}$.

3. NUMERICAL PROCEDURE

The above analysis has been incorporated into the DASAB code in order that load-deflection curves required in design applications can be readily computed. Salient features of this program are:

1. Use of an iteration technique rather than an incremental procedure to find the deflected shape of a fuel bundle subjected to a prescribed combination of concentrated and/or uniform loads. Barinka [1] has indicated that his analysis employs a step-by-step iteration procedure at each coupling location with the loading applied in small increments until the load level of interest is attained. In the present code, only the desired load level is specified and a nested iteration procedure is then employed at each coupling location to ascertain the required value of the interaction force ($r^h_{f,i}$) and interaction moment ($m^c_{f,i}$). The slippage behavior in the present model follows the pattern outlined in [1] (initial slippage at outer rows in the interior of the bundle which, with application of more load, spreads toward the centerline and boundaries of the bundle).
2. Complete flexibility in the specification of boundary conditions via an input parameter which designates the spring modulus K(K=0 is the case investigated in [1] i.e., pinned ends; whereas, K=∞ designates clamped ends) corresponding to rotational springs at the bundle supports. The deflected shape of a given fuel bundle with a designated degree of end fixity is computed with the aid of a numerical subroutine that solves a general nonlinear equation of the form f(X)=0 by means of Mueller's iteration method (See-Kristiansen [4]). Input parameters required in this subroutine specify the maximum number of iteration steps to be

employed, an upper bound on the error of the solution, left (X_ℓ) and right (X_r) boundaries on the argument X and the name of the function routine, f(X), to be evaluated by Mueller's method. An additional requirement of the iteration scheme is that the product of $f(X_\ell)$ and $f(X_r)$ be less than or equal to zero. This restriction is a necessary condition for the numerical procedure to converge on the value of X required to satisfy f(X)=0.

3. Computation of the deformed bundle configuration by the following technique

   a. Specification of the initial geometry, loading, interaction spring constants and support conditions as data to be read into the program.
   b. Calculation of the statically determinate vertical reactions at the supports and an estimated value of the moment at the supports required to produce a specified end fixity. For pinned supports the moments (M_p) are known to be zero and for rotationally constrained supports the applied moment (M_a) is assumed to satisfy the expression $M_p<M_a<M_c$ where M_c is the support moment for a clamped beam with a length and loading identical to that of the fuel bundle.
   c. Computation of the values of $f(X_\ell)$ and $f(X_r)$ associated with the specified end moments. The arguments of f are the lower and upper bounds, respectively, on the applied end moments required to produce the designated end fixity. Thus for pinned ends $f(X)=f_p(0)$ since $X_\ell=X_r=M_p=0$ and for non-zero end moments $X=M_p$ and $X_r=M_c$. For clamped supports, the function $f(X)=f_c(X)$ is defined to be the angle of bundle rotation at the boundaries and for constrained supports with a finite rotational spring modulus, $f(X)=f_{rc}(X)$ is equated to the difference between the calculated and specified spring constant divided by the absolute value of the specified spring constant. Because the iteration procedure described in Step 2 is utilized in the case of non-zero rotational constraint, the product of $f(X_\ell)$ and $f(X_r)$ is evaluated in these cases. If the result is not less than or equal to zero, the value of X_r is modified until the stipulated condition is satisfied. For a designated argument, evaluation of f(X) is accomplished by employing a technique similar to the spanwise computational cycle described in [1]. This procedure consists of an iteration loop which starts at the midspan of the bundle and, for each succeeding bundle segment, computes the desired twelve unknowns. Significant computations for segment i include determination of the total segment shear (Q_i) and the total segment moment (M_i) from equilibrium considerations, calculation of both invariant and slippage dependent matrix coefficients, solution for the desired unknowns via matrix inversion and checking of slippage criteria with modification of appropriate matrix coefficients and repeated matrix inversion until a satisfactory solution is obtained. Upon completion of the iteration loop, the angle of bundle rotation at the support is utilized to compute f(X) for rotationally constrained bundles. For pinned supports, the function routine, f(X), is called only once with argument zero. The computed deformation is the desired solution and the program returns from the function routine without computation of a value of f(X) for subsequent use in Mueller's iteration method.
   d. Determination of the applied moments (for non-zero K) necessary to produce the specified K. This is accomplished by employing the bending moments X_ℓ and X_r, ascertained in (c), in the subroutine containing Mueller's iteration scheme. As previously indicated, this step is omitted for pinned bundles.
   e. Computation of the total deflection of the bundle at the end of each segment. The desired deflection curve across the length of the bundle is calculated by substituting the incremental deformations computed in (c) or (d) into (17) or (18).

4. NUMERICAL RESULTS

To illustrate the influence of the boundary conditions on the deflection of a fuel bundle, the load versus maximum deflection curves for a hypothetical fuel bundle were computed for four different boundary conditions. In addition to the boundary conditions, the bundle parameters shown in Table 1 were specified as input to the DASAB code. The computed numerical results are summarized in Figure 5. The significant effect of the boundary conditions on the bundle deflection is seen by comparing the maximum deflection of the pinned bundle to that of the clamped bundle for a transverse concentrated load at midspan of 50 pounds. The ratio of the deflection in the pinned bundle to that in the clamped is 9.6; whereas, the corresponding ratio for a classical elastic beam is 4. For this loading, fuel rod slippage occurs at 8(4) coupling locations and at all 18 cross section elevations for the pinned (clamped) bundle. Because the center grid is the computational datum, the maximum number of possible slippage sites is 144 (8x18). Thus, additional reduction in moment resistance due to rod slippage is not possible for the pinned bundle since this number has been attained. An index of the reduction in rotational constraint is defined by assigning to the coupling location the digit in the vertical component of the slope of the segment in Figure 4 utilized in the deformation calculations ($K\theta 1$ yields an index of 1, etc.) at a given coupling location. The maximum value that can be obtained from summing these indices is 32(8x4) and the corresponding values for the pinned and clamped bundles loaded by the 50 pound load are 28 and 18, respectively. This demonstrates that the two nonlinear mechanisms incorporated in the model exert appreciable influence on the deformation at higher load levels. Also, as stated earlier, a desired end fixity cannot be prescribed by specifying the corresponding moment calculated from simple beam theory to the bundle supports. For example, a moment of 1746.76 inch pounds is required in order to achieve clamped boundaries on the present bundle. This rotational restraint is significantly larger than the 1250 inch pound moment at the clamped supports of an elastic beam with a span equal to that of the fuel bundle.

5. NOMENCLATURE

A_j - Cross sectional area of tube type j

E_j - Young's modulus for tube type j

f_o - exterior surface force required for fuel rod slippage

h - superscript indicating the tube row on cross section (h=1 corresponds to the row with the most negative Z coordinate)

i - subscript denoting coupling station

I_j - moment of inertia of tube type j

j - subscript denoting tube type

KX_j - constant relating exterior surface force to relative axial motion between the spacer grid and tube type j

$K\theta_j$ - constants relating exterior surface moment to relative angular motion between the spacer grid and tube type j

L_i - length of fuel bundle segment i

M_i - total moment applied to fuel bundle segment i

$M_{j,i}$ - moment applied to tubes of type j at cross section i

$m_{j,i}$ - internal moment in an individual tube of type j at cross section i

$m'_{j,i}$ - moment on the exterior surface of an individual tube of type j at cross section i

$m_o(\ )$ - values of the exterior surface moment at the juncture of linear segments in Figure 4

N_j - total number of tubes of type j in the fuel bundle

N_j^h - number of tubes of type j in row h of the cross section

NRJ - number of rows of tubes of type j in the cross section

NRS - number of the row of fuel rods nearest the neutral axis in the lower helf of the cross section where tube slippage has occurred.

Q_i - total shear applied to the fuel bundle segment i

$Q_{j,i}$ - shear applied to tubes of type j at cross section i

$q_{j,i}$ - transverse internal force in an individual tube of type j at cross section i

$q'_{j,i}$ - transverse force on the exterior surface of an individual tube of type j at cross section i (assumed to be zero in this study)

$r^n_{j,i}$ - axial internal force on an individual tube of type j at cross section i

$r^h_{j,i}$ - axial force on the surface of an individual tube of type j at cross section i

w_j - uniform load applied to tube j

$Z^h_{j,i}$ - transverse cross section coordinate of tube row h for tube type j

$\Delta X^h_{j,i}$ - axial displacement of tube row h for tube type j at cross section i

$\Delta Y_{j,i}$ - transverse displacement of tube type j at cross section i

$\Delta\theta_{j,i}$ - angular rotation of tube type j at cross section i

$\Delta\theta^P_{j,i}, \Delta\theta^N_{j,i}$ - values of the angular rotation of tube type j at cross section i corresponding to the m_o values of Figure 4

$\delta X^h_{j,i}$ - axial displacement of grid location h for tube type j at cross section i

$\delta\theta_{j,i}$ - angular rotation of the grid associated with tube type j at cross section i

$\delta\theta^P_{j,i}, \delta\theta^N_{j,i}$ - values of the angular rotation of the grid associated with tube type j at cross section i corresponding to the m_o values of Figure 4

$\theta_{j,i-1}$ - total angular rotation the grid associated with tube type j at cross section i-1

6. REFERENCES

1. Barinka, L. L., "Nonlinear Deflection Analysis for Coupled Tubular Structures", Journal of Engineering for Industry, Nov. 1971, pp. 1255-1260.

2. Halliday, K. L. and Horvay, G., "Deflection Analysis of a Nuclear Reactor Fuel Rod Assembly", Proceedings of the 3rd International Conference on Structural Mechanics in Reactor Technology, London, Sept. 1975.

3. Popov, E. P., "Mechanics of Materials", Prentice-Hall, Inc., Englewood Cliffs, N. J., 1958, p. 283.

4. Kristiansen, G. K., "Zero of an Arbitrary Function", Bit, Vol. 3, 1963, pp. 205-206.

TABLE 1 - FUEL BUNDLE PARAMETERS

Bundle length	200 inches
Number of Coupling Locations	Nine equally spaced (excludes supports)
Young's Modulus-Guide Tubes	15×10^6 lb/in^2
Young's Modulus-Fuel Rods	15×10^6 lb/in^2
Outer Radius-Guide Tubes	0.3125 inches
Inner Radius-Guide Tubes	0.3000 inches
Outer Radius-Fuel Rods	0.2250 inches
Inner Radius-Fuel Rods	0.2000 inches
Cross Section Composition	216 Tubes in 18 rows of 12 tubes each. Located at intervals of 0.5 inches above and below the neutral axis (maximum coordinate 4.5 inches and minimum coordinate-4.5 inches)
Location of Guide Tubes	2(2) tubes located 2 inches above(below) the neutral axis. Tubes situated equi-distant from the vertical axis of symmetry of the cross section
Location of Fuel Rods	remaining vacancies in 18x12 matrix
$K\dot{X}$ for Guide Tubes	1×10^{20} lb/in
KX for Fuel Rods	3×10^4 lb/in
f_o for Fuel Rods	1 lb
K01 for Guide Tubes	5×10^4 lb-in/rad
K01,K02,K03,K04 for Fuel Rods	2500,1250,625 and 0.001 in-lb/rad, respectively
mo(1),mo(2),mo(3),mo(4),mo(5) for Fuel Rods	0,1,2,3,and 4 in-lb, respectively

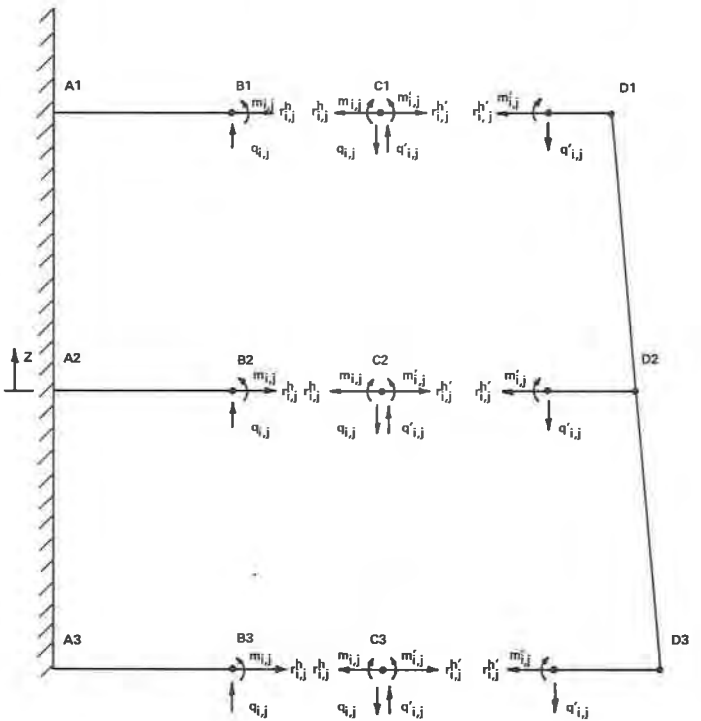

FIGURE 1

DIAGRAMMATIC REPRESENTATION OF A BUNDLE SEGMENT

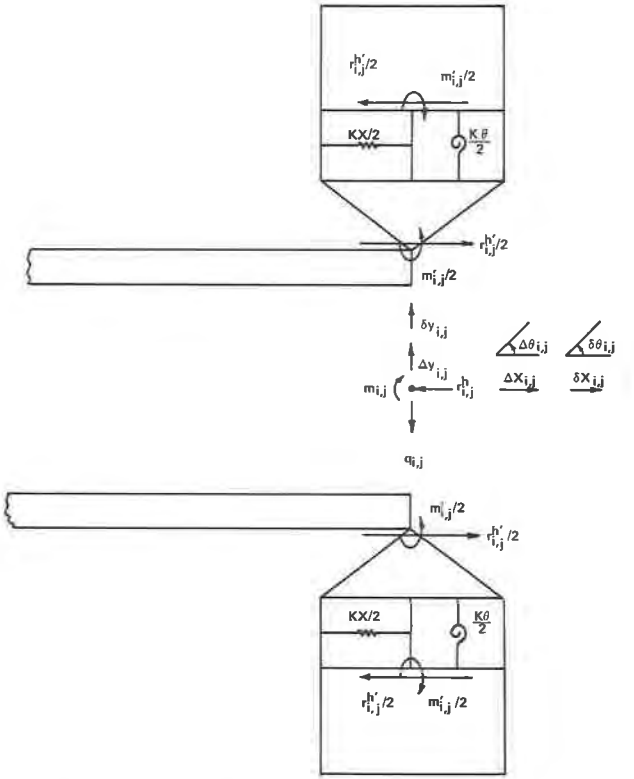

FIGURE 2 INTERNAL AND EXTERNAL FORCES AT A COUPLING JOINT

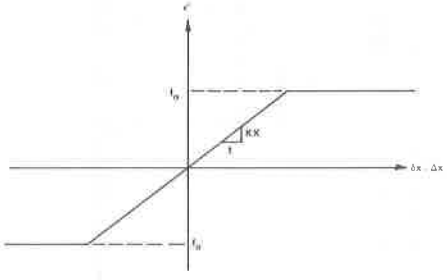

Figure 3

EXTERNAL COUPLING FORCE VERSUS RELATIVE AXIAL DISPLACEMENT

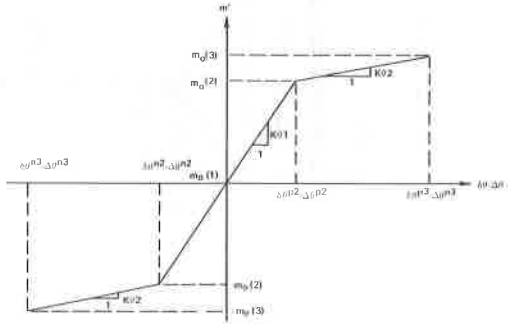

Figure 4

EXTERNAL COUPLING MOMENT VERSUS RELATIVE ROTATION

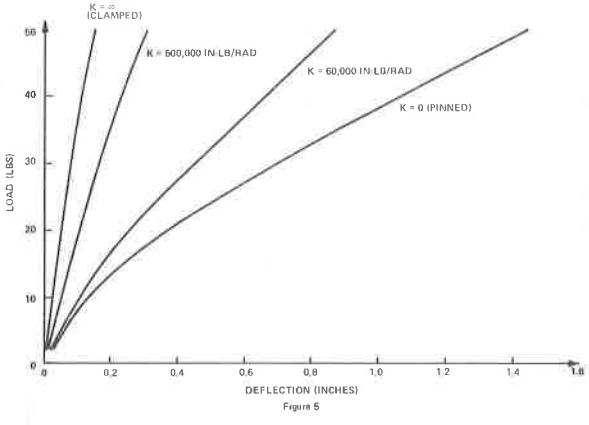

Figure 5

LOAD DEFLECTION CURVES FOR CENTRALLY LOADED 18 x 12 FUEL BUNDLE